Test of semilocal duality in a large N_C framework

Ling-Yun Dai,[1,2,*] Xian-Wei Kang,[3,†] and Ulf-G. Meißner[2,4,5,‡]

[1]*School of Physics and Electronics, Hunan University, Changsha 410082, China*
[2]*Institute for Advanced Simulation, Institut für Kernphysik and Jülich Center for Hadron Physics, Forschungszentrum Jülich, D-52425 Jülich, Germany*
[3]*College of Nuclear Science and Technology, Beijing Normal University, Beijing 100875, China*
[4]*Helmholtz Institut für Strahlen- und Kernphysik and Bethe Center for Theoretical Physics, Universität Bonn, D-53115 Bonn, Germany*
[5]*Tbilisi State University, 0186 Tbilisi, Georgia*

(Received 20 August 2018; published 31 October 2018)

In this paper we test the semilocal duality based on the method of [L. Y. Dai and U.-G. Meißner, Phys. Lett. B **783**, 294 (2018)] for calculating final-state interactions at varying numbers of colors (N_C). We compute the amplitudes by dispersion relations that respect analyticity and coupled channel unitarity, as well as accurately describing experiment. The N_C dependence of the $\pi\pi \to \pi\pi$ scattering amplitudes is obtained by comparing these amplitudes to the ones of chiral perturbation theory. The semilocal duality is investigated by varying N_C. Our results show that the semilocal duality is not violated when N_C is large. At large N_C, the contributions of the $f_2(1270)$, the $f_0(980)$ and the $f_0(1370)$ cancel that of the $\rho(770)$ in the finite energy sum rules, while the $f_0(500)$ has almost no effect. This gives further credit to the method developed in [L. Y. Dai and U.-G. Meißner, Phys. Lett. B **783**, 294 (2018)] for investigating the N_C dependence of hadron-hadron scattering with final-state interactions. This study is also helpful to understand the structure of the scalar mesons.

DOI: 10.1103/PhysRevD.98.074033

I. INTRODUCTION

The $1/N_C$ expansion [1,2] provides an effective diagnostic to differentiate the ordinary from the nonordinary quark-antiquark structure of the mysterious scalars; see e.g., [3–7]. In the physical world, i.e., at $N_C = 3$, there should be local duality [8–13]. This means that Regge exchange in the crossed channel is dual to the contribution of resonances in the direct channel. One thus only needs to add either the Regge term or the direct channel resonances in a given calculation. An explicit model shows that there is no interference between these two contributions [8]. Indeed, in the high-energy region the overlap of the resonances is much stronger, leading to a smooth amplitude. Such a smooth amplitude is similar to the one generated by Regge poles in the t-channel. The cross section is therefore more readily described by the Regge exchange in the crossed channel rather than by lots of resonances in the direct (s-) channel. However, in the real world, things are more complicated as the widths of the resonances are finite and only semilocal duality is fulfilled [6]. Through finite-energy sum rules (FESR) the equivalence between the resonances in the direct s-channel and the Regge poles in the crossed t-channel holds on the average [11,12].

In the pioneering work of [6], the semilocal duality is tested in the large N_C case and it is shown to be useful for investigating the structure of the light scalar mesons. The scattering amplitudes are obtained by unitarized chiral perturbation theory (UχPT) and the N_C dependence of the pertinent low-energy constants is taken over to the amplitudes. The FESR are tested by tuning N_C up to 30 or 100. They found that the $f_0(500)$ (often also called the σ) should contain a subdominant $\bar{q}q$ component and this ensures that the semilocal duality is fulfilled up to $N_C =$ 15–30. This was later used to constrain the meson-meson scattering amplitudes calculated within $U(3)$ unitary χPT [14]. The semilocal duality could be fulfilled very well up to $N_C = 30$. The relation between local duality and exotic states is also discussed in Ref. [15].

On the other hand, final-state interactions (FSI) play an important role in hadron phenomenology, especially when the energy is not very far away from the threshold of a pair or triplet of hadrons. For different models to describe the FSI, see e.g., [16–28]. In our earlier paper, a new method to study the large N_C behavior of the FSI was proposed [29].

*l.dai@fz-juelich.de
†kangxianwei1@gmail.com
‡meissner@hiskp.uni-bonn.de

The N_C dependence is generated based on the fact that the tangent of the phase is proportional to $1/N_C$, that is, $\tan\varphi \sim \mathcal{O}(1/N_C)$, where $\mathrm{Re}T \sim \mathcal{O}(1/N_C)$ and $\mathrm{Im}T \sim \mathcal{O}(1/N_C^2)$ are naturally given by chiral perturbation theory (χPT). The trajectories of the widths of the ρ and the f_2 quantitatively behave as $1/N_C$, which confirms the reliability of the method. Following that work, a natural extension is to check whether the semilocal duality is satisfied using this method.

This paper is organized as follows: In Sec. II we use a dispersive method to obtain the $I = 2$ $\pi\pi$ scattering partial waves up to $s \sim 4$ GeV^2, which were not considered in [29]. The amplitudes are constructed analytically and respect the coupled channel unitarity and give a good description of the experimental data. In Sec. III we introduce the N_C dependence into the dispersive amplitudes following Ref. [29]. The semilocal duality is tested by tuning N_C up to 180. We find that it works well when N_C is large. The contributions of each resonance that appear in the amplitudes are also studied. Finally we give a brief summary in Sec. IV.

II. SCATTERING AMPLITUDES AND N_C DEPENDENCE

In Ref. [29], the $\pi\pi$ scattering amplitudes with $IJ = 00$, 11, 02 (with I/J the total isospin/angular momentum) have already been given. Here, we focus on the isospin-2 waves with $IJ = 20$, 22 to complete the analysis. All these waves are certainly needed for testing the semilocal duality. We use (for more details on the method, see [29])

$$T_J^I(s) = P_J^I(s)\Omega_J^I(s), \tag{1}$$

with $\Omega_J^I(s)$ the Omnès function [30]:

$$\Omega_J^I(s) = \exp\left(\frac{s}{\pi}\int_{4M_\pi^2}^{\infty} ds' \frac{\varphi_J^I(s')}{s'(s'-s)}\right). \tag{2}$$

Here, $\varphi_J^I(s)$ is the phase of the partial wave amplitude $T_J^I(s)$, as given in previous amplitude analysis [31,32]. By a fit to the experimental data [33] as well as the amplitudes of the dispersive analysis [34], the phase is obtained up to $s = 4$ GeV^2. Above this energy region we use unitarity to constrain it, but for practical reasons the extension is limited and we truncate the integration of the Omnès function at $s = 22$ GeV^2. The other function $P_J^I(s)$ is represented by a series of polynomials. It absorbs the contribution from the left-hand cut (l.h.c.) and the distant right-hand cut (r.h.c.) above 4 GeV^2. To include the Adler zero in the S-wave and threshold behavior in the D-wave, in terms of the scattering length and effective range, we parametrize the $P_J^I(s)$ as

$$P_J^I(s) = (s - z_J^I)^{n_J}\sum_{k=1}^{n}\alpha_{J\,k}^I(s - 4M_\pi^2)^{k-1}, \tag{3}$$

TABLE I. The fit parameters corresponding to Eq. (3). The uncertainties are given by MINUIT and $\alpha_{1,2}$ are fixed by the scattering lengths and slope parameters [34,35].

	$T_0^2(s)$	$T_2^2(s)$
α_1	−1.2489	0.0472
α_2	2.1544	−0.4514
α_3	−3.2683(7)	1.1773(1)
α_4	3.2207(3)	−1.5165(1)
α_5	−1.8749(1)	1.0138(1)
α_6	0.6212(1)	−0.3587(1)
α_7	−0.1077(1)	0.0638(1)
α_8	0.0076(1)	−0.0045(1)

with z_J^I to be either the Adler zero for the S-wave or $4M_\pi^2$ for the D-wave. Similarly, n_J is 1 for the S-wave and 2 for the D-wave. The fitted parameters α_i are given in Table I. The units of the α_k are chosen to guarantee the amplitude $T_J^I(s)$ to be dimensionless.

The fit amplitudes are shown in Fig. 1 for the energy region of $s \in [0, 4\ \mathrm{GeV}^2]$. What we fit to are the following contributions: χPT amplitudes for $[0, 4M_\pi^2]$ [36–39], amplitudes of the Roy-type equation analysis at $[4M_\pi^2, 2\ \mathrm{GeV}^2]$ [34], and experiment up to 4 GeV^2 [33]. We also plot the amplitudes in the region of $s \in [-4M_\pi^2, 0]$. Here the real part of our amplitudes is in good agreement with that of χPT [$\mathcal{O}(p^4)$], and the imaginary part vanishes, which is consistent with the imaginary part of the χPT amplitudes as the latter is rather small. These indicate the high quality of the fit.

As is well known, the Roy-type equation analysis embodies crossing symmetry,[1] which is lacking in Eq. (1). Therefore, following [41], we fit our amplitudes to the "data" on the real axis as well as the amplitudes given by the Roy-like equation [34] in the complex s-plane. As shown in Fig. 2, the two T_0^2 amplitudes are compatible with each other except for the region where s is too large (either $\mathrm{Re}[s] > 1.0$ GeV^2 or $\mathrm{Im}[s] < -0.3$ GeV^2). We note that the amplitudes on the upper half of the s-plane are readily obtainable from the ones on the lower side according to the Schwarz reflection principle. The distribution of contours is in good agreement and moreover, their gradient variations are compatible with each other, as shown by the shading of the color from blue to red. Nevertheless, above 1.0 GeV our amplitudes are a bit different from that of the dispersive analysis, while both of them are compatible with the data; see Fig. 1. Also our amplitudes in the bottom-right direction, where either $\mathrm{Re}[s]$ or $\mathrm{Im}[s]$ is large, are becoming less consistent with differences $\lesssim 0.1$.

Now that these amplitudes are obtained for the physical world, that is for $N_C = 3$, we can introduce the N_C

[1]Notice that the D-wave is absent in the Roy-like equation analysis [34] and the $I = 2$ D-wave is very small; we thus do not discuss it here. For higher partial waves we refer to Ref. [40].

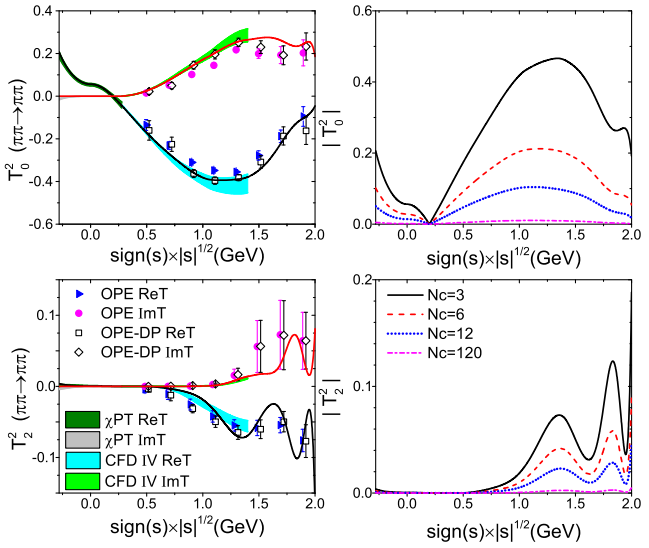

FIG. 1. Left column: Fit of the isospin-2 $\pi\pi$ scattering amplitudes (solid lines). The olive and light grey bands in the low-energy region are from χPT [36–39]. The cyan and green bands are from CFDIV [34]. The OPE and OPE-DP data are from [33]. Right column: The absolute values of the amplitudes by varying N_C are shown. The black solid, orange dashed, blue dotted and magenta dashed-dotted lines are for $N_C = 3$, 6, 12, 120, respectively.

dependence. Apparently, the real part of the χPT amplitude is $\mathcal{O}(N_C^{-1})$ and the imaginary part is $\mathcal{O}(N_C^{-2})$ up to any order. Therefore, we generate the N_C dependence as [29]

$$\varphi(s, N_C) = \arctan\left[\frac{3}{N_C}\tan\varphi(s)\right], \tag{4}$$

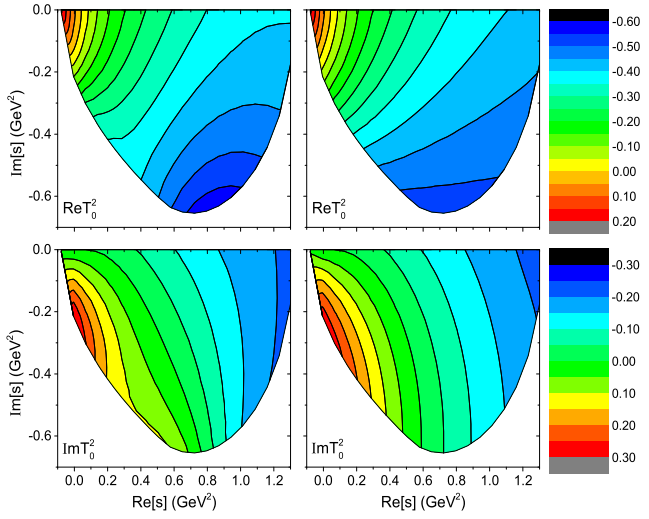

FIG. 2. Comparison of our amplitudes ($IJ = 20$) with the ones from the Roy-like equation analysis in the domain where the Roy equations work. On the left side there are real and imaginary parts of our amplitudes, and on the right side those are from Roy-like equations [34].

and

$$P_J^I(s, N_C) = \frac{3}{N_C} P_J^I(s). \tag{5}$$

It is not difficult to check that at large N_C the phase, which would return back to the phase shift in a single channel, will jump by π around $s = M_R^2$ where $\varphi(M_R^2) = 90°$. This is consistent with the large N_C property of a simple Breit-Wigner formalism or the "narrow resonance pole" on the second Riemann sheet [42]. All the complicated higher-order N_C dependence is ignored for simplicity. By increasing N_C, the magnitude of the $I = 2$ S-wave and D-wave become smaller and smaller, as shown in Fig. 1. This is consistent with the fact that there is no resonance in the $I = 2$ channel.

III. SEMILOCAL DUALITY

We follow Ref. [6] to calculate the variation of the FESR by tuning N_C. It is well known that the t-channel $\pi\pi$ scattering amplitudes could be written in terms of the s-channel ones according to the crossing relations

$$T^{I_t}(s, t) = \sum_{I_s'=0}^{2} C_{st}^{I_t I_s'} T^{I_s'}(s, t),$$

where I denotes the total isospin ($I = 0$, 1, 2) of the $\pi\pi$-system and C_{st} is the orthogonal crossing matrix

$$C_{st} = C_{ts} = \begin{pmatrix} 1/3 & 1 & 5/3 \\ 1/3 & 1/2 & -5/6 \\ 1/3 & -1/2 & 1/6 \end{pmatrix}. \tag{6}$$

The s-channel amplitude is composed of a complete set of partial waves

$$T^{I_s}(s, t) = \sum_J (2J + 1) T_J^{I_s}(s) P_J(\cos\theta_s),$$

with θ_s the s-channel scattering angle in the center of mass frame. Of course, $I_s + J$ should be even as required by Bose symmetry and isospin conservation. Higher partial waves are less known and we restrict our amplitudes up to the D-waves.

We introduce the function

$$F_n^{I_t}(\nu, t) = \mathrm{Im} T^{I_t}(\nu, t) \nu^{-n}, \tag{7}$$

with $\nu = (s - u)/2$. We note that when $t = 4M_\pi^2$, $\nu = s = -u$. Semilocal duality implies that the contribution of Regge exchange and of resonances are dual with each other on the average,

TABLE II. Comparison of the $R_n^{I_t}(t)$ ratios between our amplitudes and that of Regge exchange. The latter is given by [6]. S,P,D represent our work up to the D-waves, and S,P represent our work with only S- and P-waves.

		$I_t=0$		$I_t=1$	
	n	$t=4M_\pi^2$	$t=0$	$t=4M_\pi^2$	$t=0$
S,P,D	0	0.431(116)	0.430(122)	0.381(162)	0.396(183)
	1	0.656(85)	0.668(85)	0.619(131)	0.649(139)
	2	0.842(40)	0.865(34)	0.829(73)	0.866(69)
	3	0.948(12)	0.968(8)	0.948(32)	0.973(26)
S,P	0	0.626(201)	0.599(179)	0.779(404)	0.770(384)
	1	0.801(148)	0.793(130)	0.893(278)	0.896(252)
	2	0.914(74)	0.921(59)	0.957(132)	0.964(104)
	3	0.972(26)	0.982(17)	0.987(46)	0.993(29)
Regge	0	0.225	0.233	0.325	0.353
	1	0.425	0.445	0.578	0.642
	2	0.705	0.765	0.839	0.908
	3	0.916	0.958	0.966	0.990

$$\int_{\nu_1}^{\nu_2} d\nu F_n^{I_t}(\nu,t)_{\text{resonances}} \simeq \int_{\nu_1}^{\nu_2} d\nu F_n^{I_t}(\nu,t)_{\text{Regge}}. \quad (8)$$

To test duality in the large N_C limit, we first estimate it at $N_C=3$. It is helpful to introduce the ratio [6]

$$R_n^I(t) = \frac{\int_{\nu_1}^{\nu_2} d\nu F_n^{I_t}(\nu,t)}{\int_{\nu_1}^{\nu_3} d\nu F_n^{I_t}(\nu,t)}. \quad (9)$$

The upper and lower limits of the integration are chosen as $\nu_1=(4M_\pi^2+t)/2$, $\nu_2=1$ GeV^2, and $\nu_3=2$ GeV^2. The $R_n^I(t)$ of our amplitudes and that of the Regge amplitudes are given in Table II. As can be seen, our calculation with the D-waves is compatible with that of Regge exchange [6] within the uncertainties. For more discussions about the Regge analysis, we refer to [6].[2]

The difference between the Regge and our amplitudes as well as the difference between our two results (with or without D-waves) are much more obvious at $n=0$ than those at $n=3$. This tells us that the D- and even higher partial waves cannot be ignored at small n. In contrast, for large n the low-energy amplitudes will dominate the integration and the contribution of resonances could be less important. We thus pay attention to $n=1$–3 only and include the D-waves in the next sections. As a support, the $R_n^I(t)$ of the Regge analysis and ours (with D-waves) are closest to each other for $n=2$, 3. Also we find that the F-waves have tiny contributions only.

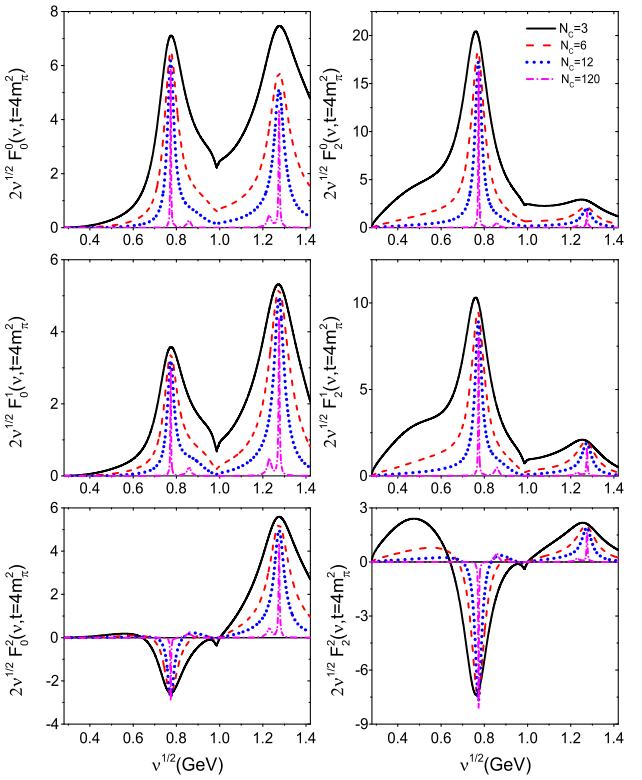

FIG. 3. The $F_n^{I_t}(\nu,t)$ amplitudes for different values of N_C; see Eq. (10). Since $\int d\nu F_n^{I_t}(\nu,t)=\int d\sqrt{\nu}2\sqrt{\nu}F_n^{I_t}(\nu,t)$, we plot $2\sqrt{\nu}F_n^{I_t}(\nu,t=4M_\pi^2)$ here.

It is instructive to plot each $F_n^I(\nu,t)$ amplitude for different values of N_C; see Fig. 3. Notice that the peaks around $\sqrt{\nu}=0.85$, 1.25 GeV at $N_C=120$ are caused by the $IJ=00$ wave; cf. Fig. 1 of Ref. [29]. They are related to the $f_0(980)$ and the $f_0(1370)$ in the large N_C limit, respectively. From Fig. 3 one notices that when n is large and N_C is not too large, the low energy amplitudes (including the σ), and the ρ have much larger contributions, while the $f_2(1270)$ contributes most at $n=0$. Only in the $I_t=2$ amplitude is the contribution of the ρ negative, which will cancel other contributions such as those from the σ in the low-energy region and from the $f_2(1270)$ in the high-energy region. This makes sure that $F_n^{I_t=2}(\nu,t)$ is superconvergent, being much smaller than the corresponding function for $I_t=0$ or $I_t=1$. Note that resonances/Regge exchanges are built from $q\bar{q}$ and multiquark contributions. When N_C is large, the pole of the $\bar{q}q$ state will fall down to the real axis on the s-plane (zero width), while the multiquark component will disappear.[3] Consequently,

[2]It is worth noting that in [6] the scattering lengths of $IJ=11$, 02 waves are calculated in the Regge parametrization with $n=2$, 3. They are in perfect agreement with that obtained by the dispersive analysis. This certainly confirms the semilocal duality at $N_C=3$, especially when $n=2$, 3. In Ref. [43] the nonlinear Regge trajectory of the $f_0(500)$ is obtained and this supports its nonordinary nature.

[3]Nowadays it is believed that tetraquarks could be as narrow as the conventional $\bar{q}q$ resonances [44] or even narrower [45]; however, these will not change our conclusion as we do not have any tetraquarks in the $I=2$ amplitude.

TABLE III. Duality by tuning N_C, given here for $N_C = 3, 6, 12, 120$.

			$\nu_{\max} = 1$ GeV^2		$\nu_{\max} = 2$ GeV^2	
	n	N_C	$t = 4M_\pi^2$	$t = 0$	$t = 4M_\pi^2$	$t = 0$
F_n^{10}	0	3	0.50(2)	0.49(2)	0.56(5)	0.53(5)
		6	0.54(2)	0.55(2)	0.68(6)	0.67(5)
		12	0.57(2)	0.58(2)	0.75(6)	0.74(6)
		120	0.59(3)	0.61(3)	0.81(6)	0.82(6)
	1	3	0.51(2)	0.51(2)	0.55(3)	0.53(3)
		6	0.55(2)	0.56(2)	0.63(3)	0.62(3)
		12	0.56(2)	0.58(2)	0.67(3)	0.67(3)
		120	0.58(3)	0.60(3)	0.71(4)	0.72(3)
	2	3	0.54(2)	0.56(2)	0.55(2)	0.55(2)
		6	0.56(2)	0.58(2)	0.60(2)	0.60(2)
		12	0.57(2)	0.59(2)	0.62(2)	0.63(2)
		120	0.57(4)	0.58(4)	0.63(4)	0.65(3)
	3	3	0.58(2)	0.63(2)	0.58(2)	0.63(2)
		6	0.59(2)	0.62(2)	0.60(2)	0.63(2)
		12	0.58(2)	0.61(2)	0.60(2)	0.62(2)
		120	0.56(4)	0.57(4)	0.59(4)	0.60(3)
F_n^{21}	0	3	−0.41(2)	−0.30(2)	0.46(5)	0.50(5)
		6	−0.40(7)	−0.29(8)	0.50(11)	0.53(13)
		12	−0.39(11)	−0.27(12)	0.53(14)	0.56(17)
		120	−0.37(14)	−0.26(14)	0.56(14)	0.59(14)
	1	3	−0.33(2)	−0.18(2)	0.17(2)	0.24(2)
		6	−0.36(8)	−0.22(9)	0.19(11)	0.25(12)
		12	−0.39(12)	−0.26(13)	0.20(15)	0.25(18)
		120	−0.45(15)	−0.34(15)	0.22(15)	0.26(16)
	2	3	−0.13(2)	0.13(2)	0.05(2)	0.24(2)
		6	−0.24(7)	−0.04(9)	−0.00(10)	0.13(11)
		12	−0.34(10)	−0.18(12)	−0.05(14)	0.05(16)
		120	−0.51(12)	−0.41(16)	−0.13(16)	−0.07(15)
	3	3	0.20(2)	0.61(2)	0.24(2)	0.62(2)
		6	0.01(7)	0.37(9)	0.07(10)	0.40(11)
		12	−0.19(9)	0.11(12)	−0.09(13)	0.17(17)
		120	−0.55(11)	−0.43(15)	−0.37(17)	−0.28(17)

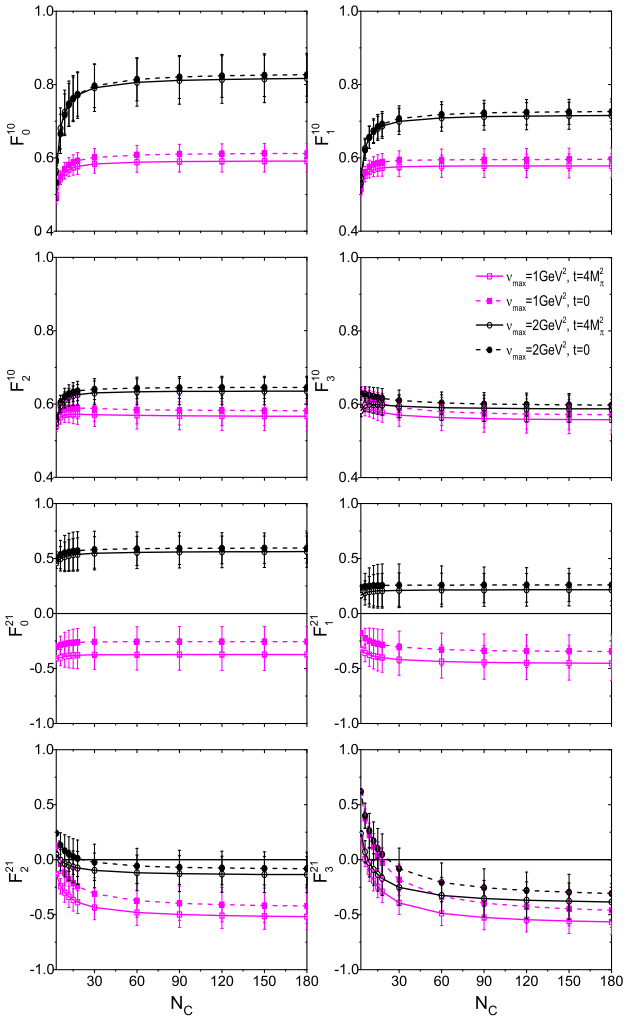

FIG. 4. Duality by varying N_C from 3 to a large number, in the order of $N_C = 3, 6, 9, 12, 15, 18, 30, 60, 90, 120, 150$ and 180.

the $I_{s/t} = 2$ amplitude is superconvergent at large N_C as it does not contain any resonances or Regge poles. Also the ratio of the $I_t = 1$ FESR compared to that of $I_t = 0$ should be $2/3$ in the large N_C limit. These are analyzed in [6] within UχPT and we will check them with our method to generate the N_C dependence in what follows.

Further, it is helpful to use the definition

$$F_n^{II'}(t) = \frac{\int_{\nu_{\min}}^{\nu_{\max}} d\nu F_n^{I_t}(\nu, t)}{\int_{\nu_{\min}}^{\nu_{\max}} d\nu F_n^{I'_t}(\nu, t)}. \tag{10}$$

As discussed before, semilocal duality means that $F_n^{10}(t)$ should be $2/3$, and $F_n^{21,20}(t)$ should be rather small. The values of these FESR for different values of N_C are given in Table III. For convenience, we plot $F_n^{10}(t)$ and $F_n^{21}(t)$ by tuning N_C up to $N_C = 180$; see Fig. 4.

Following [29], we simply assume that the whole contribution of the N_C^{-2} corrections is roughly one third of that of N_C^{-1}, while the correlation between each polynomial is not discussed, despite the fact that the first two terms of the polynomials are fixed by the scattering lengths and slope parameters. In principal, the complete separated N_C^{-2} dependence of each polynomial in Eq. (5) could be obtained by matching with χPT, if χPT is calculated up to higher orders. However, this is not yet available. One certainly needs a more careful analysis of the N_C^{-2} corrections.[4] These higher-order N_C corrections contribute most to the uncertainties at large N_C, estimated by randomly choosing $2/N_C + 3/N_C^2$ and/or $4/N_C - 3/N_C^2$ to replace $3/N_C$ in Eqs. (4) and (5) for each partial wave. The other contributions to the uncertainties are the higher partial

[4]We note that Ref. [46] points out that the subleading corrections of the low-energy constants (LECs) may be sizable as L_i/N_C, which is consistent with our assumptions. In Refs. [3,47], the uncertainty caused by the regularization scale μ is discussed, which is not required here.

waves, for instance the $IJ = 13$ wave, whose amplitude has been given in [34], and the systematic uncertainties from different solutions of the scattering amplitudes. The combination of all three parts is collected as the total uncertainty; see Table III for $N_C = 3$, 6, 12, 120. The uncertainties are also shown as error bars in Fig. 4. We note that the uncertainty of the FESR increases as N_C increases. See e.g., $F_2^{10,21}(4M_\pi^2)$ in Table III, with the upper limit $\nu_{\max} = 2$ GeV^2. This is because the uncertainty given by higher-order N_C corrections is important. Besides, the uncertainty of the $F_n^{21}(t)$ is larger than that of $F_n^{10}(t)$. The reason is that the cancellation happens at $I_t = 2$ and they are more sensitive to the relative difference between partial waves. The uncertainty coming from the upper limit $\nu_{\max} = 1$ GeV^2 is smaller than that of $\nu_{\max} = 2$ GeV^2; this is caused by the important D-waves. We will discuss this later.

The results are quite different when the upper limit is chosen to be 1 or 2 GeV^2, especially in terms of $n = 0$, 1. As an example, for $F_{0,1}^{21}(t)$ the signs of the results with these two upper limits are even opposite. For $n = 2$, 3, the differences are still distinct but smaller. This is consistent with our analysis that the $IJ = 02$ wave contributes a lot in the resonance region at small n (0 or 1). In Fig. 3, the peaks of the $f_2(1270)$ in $F_0^I(\nu, t)$ are much larger than those in $F_2^I(\nu, t)$. While at large n ($n = 2$, 3), the contribution of the $IJ = 02$ wave in the resonance region is still important but smaller. Therefore, we consider the upper limit of 2 GeV^2 as the optimal choice.

The change of the results with different n of $F_n^{10}(t)$ is smaller than that of $F_n^{21}(t)$ in the large N_C case. For example, with upper limit $\nu_{\max} = 2$ GeV^2 and $N_C = 120$, the difference between $F_0^{10}(4M_\pi^2)$ and $F_3^{10}(4M_\pi^2)$ is 0.22, while the difference between $F_0^{21}(4M_\pi^2)$ and $F_3^{21}(4M_\pi^2)$ is 0.93. The reason is that the contribution from the ρ dominates both amplitudes in $I_t = 0$ and $I_t = 1$ below 1 GeV, and the relative signs between different resonances [ρ, $f_2(1270)$ etc.] are positive, while in $I_t = 2$ the relative sign is negative; see also Eq. (6). This can be checked in Fig. 3, by comparing the lines of $2\sqrt{\nu}F_2^0(\nu, t = 4M_\pi^2)$ and $2\sqrt{\nu}F_2^1(\nu, t = 4M_\pi^2)$.

At large N_C, none of the absolute values of $F_n^{21}(t)$ is larger than 0.6, and all $F_n^{10}(t)$ are distributed in the region [0.6,0.8]. For $n = 2$, with the upper limit 2 GeV^2 and $N_C = 180$, both $F_2^{10}(4M_\pi^2) = 0.64 \pm 0.04$ and $F_2^{21}(4M_\pi^2) = -0.14 \pm 0.16$ are very close to the expected value, 2/3 and 0, respectively. Similarly, we have $F_2^{10}(0) = 0.65 \pm 0.03$ and $F_2^{21}(0) = -0.08 \pm 0.15$, even a bit closer. We note that the two kinds of results, with $t = 0$ or $t = 4M_\pi^2$, are rather similar to each other. We thus only discuss the case with $t = 4M_\pi^2$ in the next sections. For $n = 1$, 3 the situation is not so good, but the values are still fairly close to the expected values. For $n = 1$ we have $F_1^{10}(4M_\pi^2) = 0.72 \pm 0.04$ and $F_1^{21}(4M_\pi^2) = 0.22 \pm 0.15$, and for $n = 3$ we find $F_3^{10}(4M_\pi^2) = 0.59 \pm 0.04$ and $F_3^{21}(4M_\pi^2) = -0.38 \pm 0.17$. The $F_n^{21}(0, 4M_\pi^2)$ at large N_C indicates that the $f_2(1270)$ [also the $f_0(980)$ and the $f_0(1370)$] will cancel the contribution of the $\rho(770)$ most at $n = 2$. By increasing/decreasing n the cancellation is less precise, as the masses of these resonances are different. Divided by ν^n, the contributions of the ρ and that of the $f_2(1270)/f_0(980)$ are mismatched, especially around $\nu = M_R^2$. As discussed in the earlier sections, $n = 1$–3, especially $n = 2$, 3, are the most valuable cases to check the semilocal duality; one thus concludes that the results support that the semilocal duality is fulfilled well up to $N_C = 180$. There are some other points that could be interesting. Almost all the lines in Fig. 4 are increased/decreased a bit strongly from $N_C = 3$ to $N_C = 30$. One of the reasons is that the physical amplitudes are not as simple as that just represented by one or two Breit-Wigner resonances. Other components, such as multiquark components and other background, will also contribute a lot when N_C is not far away from 3. Such variation of the lines of $F_{n=2,3}^{21}(t)$ is more obvious than that of $F_{n=2,3}^{10}(t)$, where the latter is within 1/3 level. This is because the former has a strong cancellation between isospin 0 and 1 waves in the s-channel, as shown in Eqs. (6) and (7). The complex N_C relations of scalars enlarge the variation. We also notice that the lines are very flat in the region of $N_C \in [100, 180]$. It is thus natural to infer that they will stay flat for larger N_C. This suggests that the semilocal duality will hold in the large N_C limit.

To estimate the contribution of each resonance at large N_C, we perform the following calculations:

(i) *Case A*: The amplitudes of the $IJ = 00$ wave in the region of $\sqrt{s} \leq 0.75$ GeV have been set to zero. In this case the main contribution of $f_0(500)$ is removed.

(ii) *Case B*: Similar to Case A, the amplitudes of the $IJ = 00$ wave in the region of $\sqrt{s} \in [0.81, 0.91]$ GeV have been set to zero. The $f_0(980)$ is removed in the large N_C limit.

(iii) *Case C*: Similar to Case A, the amplitudes of the $IJ = 00$ wave in the region of $\sqrt{s} \in [1.13, 1.33]$ GeV have been set to zero. The $f_0(1370)$ is removed in the large N_C limit.

(iv) *Case D*: Similar to Case A, the amplitudes of the $IJ = 02$ wave in the region of $\sqrt{s} \in [1.15, 1.4]$ GeV have been set to zero. The contribution of the $f_2(1270)$ is removed.

(v) *Case E*: Only the upper limit is changed to $\nu_{\max} = 4$ GeV^2, where the possible contribution of heavier resonances, like $\rho(1450)$, $\rho(1710)$ etc. is included.

The results are shown in Table IV. For Cases A, D and E, the results by tuning N_C are plotted as magenta, black, and cyan lines, respectively, in Fig. 5. For Cases B and C, we cannot extract the contributions of the relevant resonances

TABLE IV. Duality for the different cases at $N_C = 180$ discussed in the text. Note that Case O is the original result shown in Fig. 4.

	$F_2^{10}(t)$		$F_2^{21}(t)$	
Case	$t = 4M_\pi^2$	$t = 0$	$t = 4M_\pi^2$	$t = 0$
O	0.64(5)	0.65(4)	−0.14(16)	−0.06(15)
A	0.63(7)	0.64(7)	−0.15(20)	−0.10(19)
B	0.59(8)	0.59(7)	−0.36(20)	−0.34(19)
C	0.62(8)	0.63(7)	−0.23(20)	−0.19(19)
D	0.59(3)	0.61(3)	−0.37(15)	−0.27(16)
E	0.63(8)	0.65(7)	−0.13(20)	−0.08(19)

except at large N_C, as there is no obvious peak for $f_0(980)$ and $f_0(1370)$ around $N_C = 3$. Therefore, we only show the results at $N_C = 180$; see Table IV.

For case A, we have $F_2^{10}(4M_\pi^2) = 0.63 \pm 0.07$ and $F_2^{21}(4M_\pi^2) = -0.15 \pm 0.20$ at $N_C = 180$. These satisfy the semilocal duality well. At $N_C = 3$, we have $F_2^{21}(4M_\pi^2) = -0.36 \pm 0.12$. It changes a lot compared to the original result; cf. Table III. It confirms that the σ contribution is not ignorable at $N_C = 3$, while it is smaller and irrelevant in the large N_C limit. The cancellation does not happen between the σ and $\rho(770)$ in the large N_C limit. This also suggests that σ is dominated by the non-$\bar{q}q$ structure components.

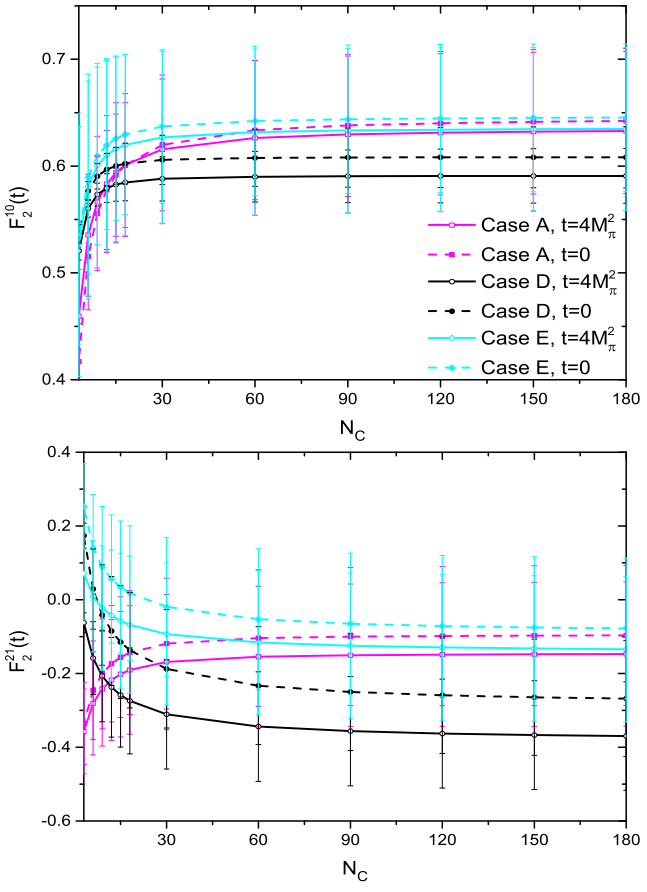

FIG. 5. Duality for the different cases defined in the text. We vary N_C from 3 to a large number, in the order of $N_C = 3$, 6, 9, 12, 15, 18, 30, 60, 90, 120, 150 and 180.

It is worth pointing out that in Ref. [14], where UχPT based on the N/D method has been applied to the meson-meson scattering of the $U(3)$ nonet, the $f_0(980)$ contribution cannot be ignored to cancel the contribution of ρ. In contrast, in Ref. [6], where UχPT is realized by an inverse amplitude method, the $f_0(980)$ is irrelevant and a subdominant $\bar{q}q$ component is needed for the cancellation. For the $f_0(1370)$, both of these two works agree as the resonance does not contribute a lot at large N_C. In our case, the two resonances behave as "peaks" around 0.85 and 1.23 GeV at large N_C, respectively. This supports their possible inner $\bar{q}q$ component, resulting in a possible contribution to cancel the ρ in $F_n^{21}(t)$. We find numerically for case B, where the contribution of the $f_0(980)$ has been removed at large N_C, that $F_2^{10}(4M_\pi^2) = 0.59 \pm 0.08$ and $F_2^{21}(4M_\pi^2) = -0.36 \pm 0.20$ at $N_C = 180$. Compared to the original results (case O), the value of $F_2^{10}(0, 4M_\pi^2)$ changes a bit, and that of $F_2^{21}(0, 4M_\pi^2)$ changes a lot. Thus, the contribution of the $f_0(980)$ at large N_C cannot be ignored. For case C, by removing the $f_0(1370)$ at large N_C, the change is smaller than that of case B but still distinct; see Table IV. This implies that the $f_0(980)$ and the $f_0(1370)$ have a significant $\bar{q}q$ component and they will partly cancel the contribution of the ρ.

In case D the $f_2(1270)$ has been removed. One finds $F_2^{10}(4M_\pi^2) = 0.59 \pm 0.03$ and $F_2^{21}(4M_\pi^2) = -0.37 \pm 0.15$ at $N_C = 180$. The $f_2(1270)$ contribution is rather important to cancel that of the ρ, just as expected. The result of case D is rather close to that of the $f_0(980)$ at large N_C, implying the same important contribution of the $f_0(980)$ as the $f_2(1270)$. In case E we consider the FESR with the upper limit $\nu_{\max} = 4$ GeV^2. The result at $N_C = 180$ is almost the same as that of case O. This supports the view that the $\rho(1450)$ as well as other heavier resonances do not have a large effect. In Fig. 5 one clearly sees that in case D the $F_2^{10}(t)$ and $F_2^{10}(t)$ deviate much more from the expected values than those in cases A and E. This confirms that the $f_2(1270)$ has a much larger effect than the $f_0(500)$ and heavier resonances such as the $\rho(1450)$.

IV. SUMMARY

In this paper we have studied the semilocal duality for large N_C. The isospin-2 $\pi\pi$ scattering amplitudes with final-state interactions are constructed in a model-independent way and fit to the data. Comparing with the amplitudes of χPT, we generate the N_C dependence of the amplitudes. With this N_C dependence the semilocal duality in terms of finite energy sum rules is tested. Our results show that the semilocal duality is satisfied well in the

large N_C limit, at least up to $N_C = 180$. This study confirms that the method of generating the N_C dependence proposed in Ref. [29] is reliable. At large N_C, the contributions of the $f_2(1270)$ and the $f_0(980)$ are important to cancel that of the $\rho(770)$, the latter is consistent with what has been found in Ref. [14]. Also the $f_0(1370)$ contributes significantly to the cancellation. In contrast, the $f_0(500)$ (or σ) has a large effect for $N_C = 3$ and a small effect at large N_C. These support the $\bar{q}q$ component in the $f_0(980)$ and the $f_0(1370)$, but not for the σ as required in Ref. [6].

ACKNOWLEDGMENTS

We are very grateful to Professor Michael R. Pennington, who has just passed away. Through discussions with him the idea underlying this paper was generated. Helpful discussions with Professors Han-Qing Zheng and Zhi-Hui Guo are also acknowledged. This work is supported by the Deutsche Forschungsgemeinschaft (SFB/TR 110, "Symmetries and the Emergence of Structure in QCD"); the Chinese Academy of Sciences (CAS) President's International Fellowship Initiative (PIFI) (Grant No. 2018DM0034); and the VolkswagenStiftung (Grant No. 93562).

[1] G. 't Hooft, Nucl. Phys. **B72**, 461 (1974).
[2] G. 't Hooft, Nucl. Phys. **B75**, 461 (1974).
[3] J. R. Pelaez, Phys. Rev. Lett. **92**, 102001 (2004).
[4] J. R. Pelaez and G. Rios, Phys. Rev. Lett. **97**, 242002 (2006).
[5] Z. X. Sun, L. Y. Xiao, Z. G. Xiao, and H. Q. Zheng, Mod. Phys. Lett. A **22**, 711 (2007).
[6] J. R. Pelaez, M. R. Pennington, J. Ruiz de Elvira, and D. J. Wilson, Phys. Rev. D **84**, 096006 (2011).
[7] L. Y. Dai, X. G. Wang, and H. Q. Zheng, Commun. Theor. Phys. **57**, 841 (2012); **58**, 410 (2012).
[8] G. Veneziano, Nuovo Cimento A **57**, 190 (1968).
[9] R. Dolen, D. Horn, and C. Schmid, Phys. Rev. Lett. **19**, 402 (1967).
[10] R. Dolen, D. Horn, and C. Schmid, Phys. Rev. **166**, 1768 (1968).
[11] C. Schmid, Phys. Rev. Lett. **20**, 628 (1968).
[12] C. Schmid, Phys. Rev. Lett. **20**, 689 (1968).
[13] K. Shiga, K. Kinoshita, and F. Toyoda, Nucl. Phys. **B24**, 490 (1970).
[14] Z. H. Guo, J. A. Oller, and J. Ruiz de Elvira, Phys. Rev. D **86**, 054006 (2012).
[15] H. Zheng, Int. J. Mod. Phys. A **20**, 1981 (2005).
[16] K. L. Au, D. Morgan, and M. R. Pennington, Phys. Rev. D **35**, 1633 (1987); D. Morgan and M. R. Pennington, Phys. Rev. D **48**, 1185 (1993).
[17] U.-G. Meißner, Comments Nucl. Part. Phys. **20**, 119 (1991).
[18] Z. H. Guo and J. A. Oller, Phys. Rev. D **84**, 034005 (2011).
[19] L. Y. Dai, M. Shi, G. Y. Tang, and H. Q. Zheng, Phys. Rev. D **92**, 014020 (2015).
[20] C. Garc-Recio, L. S. Geng, J. Nieves, L. L. Salcedo, E. Wang, and J. J. Xie, Phys. Rev. D **87**, 096006 (2013).
[21] X. W. Kang, J. Haidenbauer, and U.-G. Meißner, J. High Energy Phys. 02 (2014) 113.
[22] X. W. Kang, B. Kubis, C. Hanhart, and U.-G. Meißner, Phys. Rev. D **89**, 053015 (2014).
[23] Y. H. Chen, J. T. Daub, F. K. Guo, B. Kubis, Ulf-G. Meißner, and B. S. Zou, Phys. Rev. D **93**, 034030 (2015).
[24] R. A. Briceno, J. J. Dudek, R. G. Edwards, and D. J. Wilson, Phys. Rev. Lett. **118**, 022002 (2017).
[25] G. Colangelo, S. Lanz, H. Leutwyler, and E. Passemar, Phys. Rev. Lett. **118**, 022001 (2017).
[26] C. Hanhart, S. Holz, B. Kubis, A. Kupść, A. Wirzba, and C. W. Xiao, Eur. Phys. J. C **77**, 98 (2017); **78**, 450(E) (2018).
[27] L. Y. Dai, J. Haidenbauer, and U.-G. Meißner, J. High Energy Phys. 07 (2017) 078.
[28] H. Y. Cheng and X. W. Kang, Eur. Phys. J. C **77**, 587 (2017); **77**, 863(E) (2017).
[29] L. Y. Dai and U.-G. Meißner, Phys. Lett. B **783**, 294 (2018).
[30] R. Omnès, Nuovo Cimento **8**, 316 (1958).
[31] L. Y. Dai and M. R. Pennington, Phys. Lett. B **736**, 11 (2014); Phys. Rev. D **90**, 036004 (2014).
[32] L. Y. Dai, V. Mathieu, E. Passemar, M. R. Pennington, and A. Szczepaniak (to be published).
[33] N. B. Durusoy, M. Baubillier, R. George, M. Goldberg, and A. M. Touchard, Phys. Lett. **45B**, 517 (1973).
[34] R. García-Martín, R. Kamiński, J. R. Peláez, J. Ruiz de Elvira, and F. J. Ynduráin, Phys. Rev. D **83**, 074004 (2011).
[35] M. M. Nagels, Th. A. Rijken, J. J. De Swart, G. C. Oades, J. L. Petersen, A. C. Irving, C. Jarlskog, W. Pfeil, H. Pilkuhn, and H. P. Jakob, Nucl. Phys. **B147**, 189 (1979).
[36] J. Gasser and H. Leutwyler, Ann. Phys. (N.Y.) **158**, 142 (1984).
[37] J. Gasser and H. Leutwyler, Nucl. Phys. **B250**, 465 (1985).
[38] J. Bijnens, G. Colangelo, and J. Gasser, Nucl. Phys. **B427**, 427 (1994).
[39] A. G. Nicola and J. R. Pelaez, Phys. Rev. D **65**, 054009 (2002).
[40] R. Kaminski, Phys. Rev. D **83**, 076008 (2011).
[41] L. Y. Dai, X. W. Kang, U.-G. Meißner, X. Y. Song, and D. L. Yao, Phys. Rev. D **97**, 036012 (2018).
[42] Z. H. Guo, J. J. Sanz Cillero, and H. Q. Zheng, J. High Energy Phys. 06 (2007) 030.
[43] J. T. Londergan, J. Nebreda, J. R. Pelaez, and A. Szczepaniak, Phys. Lett. B **729**, 9 (2014).
[44] S. Weinberg, Phys. Rev. Lett. **110**, 261601 (2013).
[45] M. Knecht and S. Peris, Phys. Rev. D **88**, 036016 (2013).
[46] T. Ledwig, J. Nieves, A. Pich, E. R. Arriola, and J. Ruiz de Elvira, Phys. Rev. D **90**, 114020 (2014).
[47] J. Nieves and E. Ruiz Arriola, Phys. Lett. B **679**, 449 (2009).